

# Cyclohexyl-octahydro-pyrrolo[1,2-a]pyrazine-Based Inhibitors of Human *N*-Myristoyltransferase-1

Kevin J. French,<sup>1</sup> Yan Zhuang, Randy S. Schrecengost, Jean E. Copper, Zuping Xia,<sup>1</sup> and Charles D. Smith

Department of Pharmacology, Penn State College of Medicine, Hershey, Pennsylvania

Received October 13, 2003; accepted December 12, 2003

## ABSTRACT

*N*-Myristoyltransferase (NMT) is an emerging therapeutic target that catalyzes the attachment of myristate to the N terminus of an acceptor protein. We have developed a medium-throughput assay for screening potential small molecule inhibitors of human NMT-1 consisting of recombinant enzyme, biotinylated peptide substrate, and [<sup>3</sup>H]myristoyl-CoA. Approximately 16,000 diverse compounds have been evaluated, and significant inhibition of NMT was found with 0.8% of the compounds. From these hits, we have identified the cyclohexyl-octahydro-pyrrolo[1,2-a]pyrazine (COPP) chemotype as inhibitory toward human NMT-1. Thirty-two compounds containing this substructure inhibited NMT-1, with IC<sub>50</sub> values ranging from 6  $\mu$ M to millimolar concentrations, and a quantitative structure-activity relationship equation ( $r^2 = 0.72$ ) was derived for the series. The most potent inhibitor (24, containing 9-ethyl-9*H*-carbazole) demonstrated competitive inhibition for the peptide-binding

site of NMT-1 and noncompetitive inhibition for the myristoyl-CoA site. Computational docking studies using the crystal structure of the highly homologous yeast NMT confirmed that 24 binds with excellent complementarity to the peptide-binding site of the enzyme. To evaluate the ability of 24 to inhibit NMT activity in intact cells, monkey CV-1 cells expressing an *N*-myristoylated green fluorescent protein (GFP) fusion protein were treated with a known NMT inhibitor or with 24. Each compound caused the redistribution of GFP from the plasma membrane to the cytosol. Furthermore, 24 inhibits cancer cell proliferation at doses similar to those that inhibit protein myristoylation. Overall, these studies establish an efficient assay for screening for inhibitors of human NMT and identify a novel family of inhibitors that compete at the peptide-binding site and have activity in intact cells.

The term protein myristoylation refers to the covalent attachment of myristic acid to specific proteins. This process has been shown to target proteins to specific subcellular membranes (Boutin, 1997), stabilize protein conformation (Chow et al., 1987; Zheng et al., 1993; Resh, 1996), and facilitate additional lipidations (Robbins et al., 1995; Yurchak and Sefton, 1995; Song et al., 1997; van't Hof and Resh, 1999). Although the reaction mainly occurs as a cotranslational event, it has been shown to occur after cleavage of some substrates (Zha et al., 2000). *N*-Myristoyltransferase (NMT; E.C. 2.3.1.97) catalyzes this addition onto the N-terminal glycine residue of specific proteins. The reaction re-

quires only myristoyl-CoA and a protein containing a suitable peptide sequence and occurs through an ordered Bi Bi mechanism (Rudnick et al., 1991; Rocque et al., 1993; Bhatnagar et al., 1998). The list of myristoylated proteins is diverse, including viral proteins, G $\alpha$  proteins, tyrosine kinases of the Src family, and nitric oxide synthase. Gene replacement studies indicate that NMT is essential for viability of *Cryptococcus neoformans* (Lodge et al., 1994). In addition, mutation or deletion of NMT results in recessive lethality in *Saccharomyces cerevisiae* (Duronio et al., 1989, 1991) and *Candida albicans* (Weinberg et al., 1995). Thus, NMT appears to be an essential enzyme in both prokaryotes and higher organisms. In humans, NMT has more complex expression patterns, including a shortened alternative splice variant lacking the ribosomal targeting sequence, which occurs in several tissue types (McIlhinney et al., 1998). Additionally, Giang and Cravatt (1998) have recently cloned and characterized a second isoform (NMT-2) that demonstrates

This work was supported by National Institutes of Health Grant R24 CA788243 (to C.D.S.).

<sup>1</sup> Current address: Apogee Biotechnology Corporation, P.O. Box 916, Hershey, PA 17033.

Article, publication date, and citation information can be found at <http://jpet.aspetjournals.org>.

DOI: 10.1124/jpet.103.061572.

**ABBREVIATIONS:** NMT, *N*-myristoyltransferase; COPP, cyclohexyl-octahydro-pyrrolo[1,2-a]pyrazine; DMSO, dimethylsulfoxide; GST, glutathione *S*-transferase; myr-phe, *N*-myristoyl-L-phenylalanine; *N*-myr-GFP, *N*-myristoylated green fluorescent protein; PBS, phosphate-buffered saline; QSAR, quantitative structure-activity relationship; GFP, green fluorescent protein; MOE, molecular operating environment; MOPP, methyl-octahydro-pyrrolo[1,2-a]pyrazine; 2-HM, 2-hydroxymyristic acid.

similar activities to NMT-1. These findings reveal that NMT is an essential enzyme whose expression and processing are complex.

Several pathogenic states are linked to undesired NMT activity. The Rous Sarcoma Virus transforms cells through expression of the tyrosine kinase p60src. Kamps et al. (1986) demonstrated that mutation of the N-terminal glycine of p60src conserves its kinase activity but blocks its ability to associate with membranes and to transform cells. The Human Immunodeficiency Virus-1 gag precursor protein undergoes *N*-myristoylation, and the inhibitor *N*-myristoyl glycyl diethylacetal results in accumulation of immature gag precursors and inhibition of viral replication (Furuishi et al., 1997). NMT also appears to play a role in cancer. Increases in NMT expression and activity have been observed in colorectal adenocarcinomas (Raju et al., 1997), gallbladder carcinomas (Rajala et al., 2000), and the murine leukemia cell line L1210 (Boutin et al., 1993). Furthermore, several protein tyrosine kinases of the Src family are well established oncogenes that require myristoylation for activity (Resh, 1994). Importantly, a number of studies have shown that c-Src is a critical regulator of human cancers, including breast carcinomas (Garcia et al., 2001). Additional studies have shown that Src may be a therapeutic target for the treatment of osteoporosis (Sawyer et al., 2001).

Because of the dependence of yeast on NMT activity for growth, the consideration of NMT as a therapeutic target has primarily focused on the development of NMT inhibitors to be used as antifungal agents. The pioneering work of Gordon and colleagues led to the design and synthesis of antifungal peptidomimetic and dipeptide analog inhibitors for *C. albicans* NMT that are selective versus human NMT while demonstrating low nanomolar potencies toward the enzyme (Devadas et al., 1995, 1997; Nagarajan et al., 1997). Other recently described inhibitors include amino acid derivatives (Boutin et al., 1993; Furuishi et al., 1997; Tabuchi et al., 1997; Cordo et al., 1999) and nonhydrolyzable myristoyl-CoA analogs (Heuckeroth and Gordon, 1989; Paige et al., 1989; Wagner and Retey, 1991). However, the development of these compounds may be limited by their poor pharmacokinetic properties. Thus, we have undertaken a project to design, synthesize, and evaluate small molecule inhibitors of human NMT. We report here the discovery of the novel chemotype cyclohexyl-octahydro-pyrrolo[1,2-*a*]pyrazine (COPP) that inhibits human NMT-1 with micromolar potency.

## Materials and Methods

Unless otherwise noted, all chemicals and reagents were purchased from Sigma-Aldrich (St. Louis, MO). The library of compounds used for screening was purchased from the ChemBridge Corporation (San Diego, CA) and was provided as individual compounds dissolved in DMSO (1 mg/ml). Specific cyclohexyl-octahydro-pyrrolo[1,2-*a*]pyrazine compounds in the library were synthesized previously as described (Likhoshervstov et al., 1993). The identities of all compounds were confirmed by NMR analyses, and high-performance liquid chromatography-mass spectroscopic analyses indicated that each was of 95% or greater purity (data not shown).

The cDNA for human NMT-1 was a kind gift from Dr. Jeffrey Gordon (Washington University, St. Louis, MO). NMT-1 cDNA was subcloned into the pGEX-5x-3 bacterial expression vector (Amersham Biosciences Inc., Piscataway, NJ), resulting in the generation of a GST-hNMT-1 fusion protein. As a control, the unmodified pGEX

vector encoding only the GST portion was used. The recombinant proteins were expressed and purified on immobilized GSH columns according to the specifications of Amersham Biosciences Inc. The column eluates containing GST or GST-hNMT-1 were then dialyzed in PBS overnight to remove glutathione and stored at  $-80^{\circ}\text{C}$  in 20% glycerol until use.

Myristoyl-L-phenylalanine was synthesized and purified as follows. Myristic acid was coupled with an equimolar amount of *N*-hydroxysuccinimide by dicyclohexylcarbodiimide in ethyl acetate at room temperature for 20 h (yield, 85%). The product was then reacted with an equimolar amount of L-phenylalanine (Sigma-Aldrich; enantiomeric excess 98%) in a 50:50 solution of tetrahydrofuran/0.1 M sodium bicarbonate at room temperature for 20 h. After acidification with 1 N hydrochloric acid (final pH,  $\sim 2$ ), the final product was a white solid crystallized from chloroform and petroleum ether (yield, 60%). The identity and purity of the product was confirmed by  $^1\text{H}$ - and  $^{13}\text{C}$ -NMR analyses. The peptide substrate,  $\text{NH}_2$ -GNAASARRK-biotin, was synthesized by the Macromolecular Core Facility at the Penn State College of Medicine using standard solid-phase synthetic techniques.

**[ $^3\text{H}$ ]Myristoyl-CoA Synthesis.** [ $^3\text{H}$ ]Myristoyl-CoA was synthesized by adding 0.1 U of *Pseudomonas* sp. Acyl-coenzyme A synthase (Sigma-Aldrich) to 200  $\mu\text{l}$  of buffer (20 mM Tris-HCl, 1 mM dithiothreitol, 10 mM  $\text{MgCl}_2$ , and 0.1 mM EGTA, pH 8.0) containing 1.3 mM Coenzyme A (lithium salt), 5.4 mM ATP, and 0.8  $\mu\text{M}$  [8,9- $^3\text{H}$ ]myristic acid (50 Ci/mmol; American Radiolabeled Chemicals, St. Louis, MO). The mixture was incubated at  $37^{\circ}\text{C}$  with shaking for 1 h, and unreacted [ $^3\text{H}$ ]myristic acid was removed by acidification and extraction with hexane. The extent of conversion to [ $^3\text{H}$ ]myristoyl-CoA was determined to be 95%, and the product was stored at  $-20^{\circ}\text{C}$  until its use.

**Assay of NMT Activity.** The NMT assays were performed in streptavidin-coated 96-well plates and consisted of the following reagents: 2  $\mu\text{g}$  of purified GST-hNMT-1 fusion protein, 23 nM  $\text{NH}_2$ -GNAASARRK-biotin (stoichiometric with the amount of bound streptavidin), 0.5  $\mu\text{l}$  of 1 mg/ml test compound in DMSO, and NMT assay buffer (30 mM Tris-HCl, pH 7.4, 0.5 mM EGTA, 0.45 mM EDTA, 4.5 mM 2-mercaptoethanol, and 0.05% Tween 20). The reactions were initiated with the addition of [ $^3\text{H}$ ]myristoyl-CoA (final concentration, 60 nM) to a final volume of 100  $\mu\text{l}$  and were incubated at  $25^{\circ}\text{C}$  with shaking for 30 min. Reactions were terminated by aspiration of the incubation mixture. The bound biotinylated peptide was washed three times with 200  $\mu\text{l}$  of 30 mM Tris-HCl containing 0.05% Tween 20 and eluted with 300  $\mu\text{l}$  of 0.1 M glycine, pH 2.8. After 1 h, the eluted peptide was transferred to scintillation vials, and the amount of bound  $^3\text{H}$  was quantified to determine NMT activity.

**Competition Assays.** The peptide substrate  $\text{NH}_2$ -GNAASARRK-biotin was bound to stoichiometric excesses of streptavidin-coated polystyrene beads (Polysciences, Warrington, PA). In all competition studies, reactions were stopped before 10% of the substrate underwent myristoylation to ensure valid kinetic analyses. For peptide competition assays, the substrate concentration was varied from 0 to 500  $\mu\text{M}$  and incubated with 5  $\mu\text{g}$  of purified GST-hNMT-1 fusion protein, 160 nM [ $^3\text{H}$ ]myristoyl-CoA, DMSO or 6  $\mu\text{M}$  24, and NMT assay buffer in a total volume of 50  $\mu\text{l}$ . Reactions were incubated at  $25^{\circ}\text{C}$  with shaking for 15 min. The beads were washed twice with assay buffer by centrifugation, transferred to scintillation vials, and  $^3\text{H}$  was quantified to determine NMT activity. For myristoyl-CoA competition assays, the peptide concentration was 100  $\mu\text{M}$ , whereas myristoyl-CoA (mixed in a 1:25 ratio with nonradioactive myristoyl-CoA) concentration varied from 0 to 20  $\mu\text{M}$ . Kinetic constants were calculated by regression analyses using the Prism 3.0 software package (GraphPad Software, San Diego, CA).

**Computational Studies.** The chemical characteristics of each compound in the COPP set were determined using the 2D QSAR descriptors as calculated by the program QuaSAR-Model in the MOE software package (version 2002.03; Chemical Computing Group Inc.,

Montreal, Quebec, Canada) running on a Dell Dimension 4500S with an Intel Pentium 4 2.0 GHz processor. These descriptors were related to the biological activity of the compounds using the IC<sub>50</sub> data for inhibition of NMT activity, along with the molecular structure of each COPP analog. Detailed information about descriptors used in the QSAR can be found at [http://www.chemcomp.com/Journal\\_of\\_CCG/Features/descrip.html](http://www.chemcomp.com/Journal_of_CCG/Features/descrip.html).

The three-dimensional structure of the yeast NMT with bound myristoyl-CoA and peptide substrate analogs [S-(2-oxo)pentadecyl-CoA and SC-58272] was obtained from the Protein Data Bank using the accession code 2nmt (Bhatnagar et al., 1998). Modeling and energy analyses were performed using the program DOCK in the MOE software package with the default parameter settings. Prior to docking of 24, the peptide analog was computationally removed, and hydrogen atoms were added to the protein. Binding site analyses were conducted within a three-dimensional docking box encompassing the entire enzyme, using simulated annealing (Monte Carlo method) and tabu search protocols. Both methods were set to optimize spatial contacts as well as electrostatic interactions as determined by the molecular mechanics force field (MMFF94). Acceptance tests were conducted at the end of each docking cycle until an optimal solution (lowest total energy) was attained.

**Cellular NMT Activity Assays.** Whole-cell assay systems for the evaluation of inhibitors of protein farnesylation, palmitoylation, and *N*-myristoylation have been recently developed in this laboratory (J. E. Copper, D. W. Dexter, and C. D. Smith, manuscript submitted for publication). In these assays, various lipidation signals have been fused onto enhanced green fluorescent protein (GFP), and these proteins are expressed by transient transfection of CV-1 cells. The subcellular localization of the modified GFPs can then be determined by fluorescence microscopy. The *N*-myr-GFP plasmid was created by fusing sequence corresponding to the N terminus of Fyn (MGCVQCKTK) to GFP using polymerase chain reaction and cloning into the pZEOSV2- expression vector (Invitrogen, Carlsbad, CA). LipofectAMINE 2000 transfection reagent (Invitrogen) was used to introduce the GFP construct into CV-1 monkey kidney cells growing on glass coverslips. The cells were incubated with 24 or the solvent (DMSO) for 48 h. Cells were fixed with 4% paraformaldehyde in PBS, mounted on slides, and epifluorescence microscopy was performed using a Nikon ECLIPSE E600 microscope at 100× magnification with excitation and emission wavelengths set at 465 and 495 nm, respectively.

**Cytotoxicity Assays.** The following human tumor cell lines were obtained from the American Type Culture Collection (Manassas, VA) and grown in Dulbecco's modified Eagle's medium containing 10% fetal bovine serum and 50 µg/ml gentamycin following standard techniques: DU145, HepG2, HT29, MCF-7, MDA-MB-231, Panc-1, SKOV3, and A-498. To determine the effects of 24 on the proliferation of the cells, cells were plated into 96-well microtiter plates and allowed to attach for 24 h. Varying concentrations of 24 were added to individual wells, and the cells were incubated for an additional 72 h. At the end of this period, the number of viable cells was determined using the sulforhodamine-binding assay (Skehan et al., 1990). The percentage of cells killed is calculated as the percent of decrease in sulforhodamine-binding compared with control cultures.

## Results

**Development of the NMT Screening Assay.** Raju et al. (1996) have shown that functional human NMT can be expressed in *Escherichia coli*, indicating that the enzyme does not require post-translational modification for activity. Therefore, we expressed human NMT-1 fused to GST (to facilitate purification) in *E. coli* to develop a medium-throughput screen for inhibitors of this enzyme (Fig. 1). NMT activity was measured using purified GST-hNMT-1, biotinylated peptide with the sequence GNAASARRK, [<sup>3</sup>H]myris-

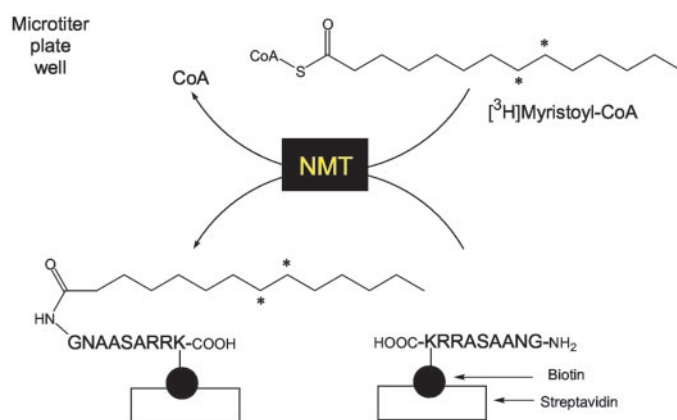


**Fig. 1.** NMT assay. Major components of the NMT activity assay are indicated, and details are provided under *Materials and Methods*. NMT represents recombinant GST-hNMT-1.

toyl-CoA, and test compound or DMSO. Conducting the assay in streptavidin-coated 96-well microtiter plates resulted in binding of the biotinylated peptide to the plates and therefore allowed rapid separation of the [<sup>3</sup>H]myristic acid substrate from the [<sup>3</sup>H]myristoylated peptide product.

The results of a typical NMT assay are depicted in Fig. 2. As shown, there was a very low background level of nonspecific binding of [<sup>3</sup>H]myristoyl-CoA to the plates (–NMT). Also, GSH column-purified lysate from *E. coli* expressing a control vector encoding GST alone showed no NMT activity. In contrast, addition of recombinant GST-hNMT-1 resulted in very large increases in bound radioactivity, thereby providing a sensitive method of detecting inhibitors. The intra-assay coefficient of variation was approximately 3%, whereas interassay variation was approximately 10%. The addition of 0.5% DMSO, the vehicle used in the chemical library, caused only a small decrease in NMT activity. A positive control, myristoyl-L-phenylalanine, was tested at the published IC<sub>50</sub> concentration of 100 µM (Boutin et al., 1991) and did in fact inhibit the recombinant human NMT by approximately 50%. An example of a hit in the screening assay, 24, is also indicated for comparison. Therefore, a sensitive and robust

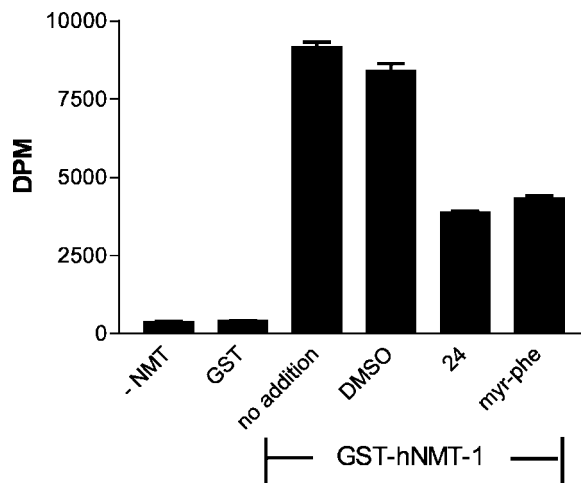


**Fig. 2.** An example of NMT assay data. The NMT assay was conducted in the absence of any recombinant (–NMT), with purified recombinant GST or with GST-hNMT-1 in the presence of DMSO, 6 µM 24, or 100 µM myristoyl-L-phenylalanine. Values represent the mean ± S.D. of NMT activity in triplicate samples in a representative experiment.



method of screening for inhibitors of human NMT has been established.

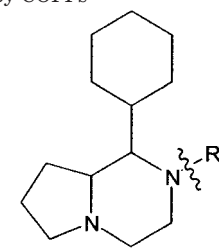
**Identification of the COPP Chemotype of NMT Inhibitors.** To facilitate screening of the compound library consisting of approximately 16,000 “drug-like” small molecules, we developed a combinatorial method in which GST-hNMT-1 was simultaneously incubated with eight compounds. Each compound was tested at a final concentration of 5  $\mu\text{g}/\text{ml}$ , which corresponds to concentrations ranging from 10 to 20  $\mu\text{M}$ . Samples that inhibited NMT activity by at least 60% were then deconvoluted, where each of the eight compounds was analyzed individually. This level of inhibition was observed in approximately 0.8% of the compounds tested. Of the approximately 120 compounds identified as inhibitors of NMT-1, a subset containing the common structure COPP was readily apparent. Substructure searching of the library database indicated that 32 compounds with the COPP chemotype and 20 containing a methyl-octahydro-pyrrolo[1,2-*a*]pyrazine (MOPP) moiety were available for analyses. These compounds were then individually tested at varying concentrations to determine their potencies for inhibiting purified hNMT-1. The  $\text{IC}_{50}$  values for inhibition of hNMT-1, along with the structures of the compounds, are listed in Table 1.

The majority of the COPP compounds had  $\text{IC}_{50}$  values near or below 100  $\mu\text{M}$ , making them adequate lead compounds for further examination. A wide range of potencies was observed, with 24 demonstrating the highest potency (6  $\mu\text{M}$ ) and six compounds being extremely weak inhibitors of NMT. MOPP compounds with similar structures but lacking the cyclohexyl moiety were mostly inactive, indicating the importance of the cyclohexyl component for inhibition of NMT (data not shown).

**QSAR Model for Inhibition of hNMT-1 by COPPs.** The number of COPP compounds evaluated was sufficient to permit ligand-based interaction analyses using QSAR. The QuasAR-Model program in the MOE software package was used to calculate a large number of two-dimensional chemical descriptors for each of the COPP compounds indicated in Table 1 and five MOPP compounds with measurable  $\text{IC}_{50}$  values (40–7300  $\mu\text{M}$ ). These descriptors were then combined with the biological data [ $-\log(\text{IC}_{50})$  for inhibition of hNMT-1] and analyzed for predictive equations using partial least-squares analyses. Through this process, a relationship between the activity of the COPP compounds and their respective structural characteristics was calculated. The optimized QSAR equation consisting of 37 descriptors is summarized in Table 2. Statistical parameters for this equation include: root mean square error, 0.50; correlation coefficient ( $r^2$ ), 0.72; cross-validated root mean square error, 1.02; and cross-validated  $r^2$ , 0.18. The relationship between the experimental and calculated  $\text{IC}_{50}$  values for inhibition of NMT is indicated in Fig. 3. All predicted  $\text{IC}_{50}$  values were within 1-log of the experimental  $\text{IC}_{50}$  values with the exception of those for 14 and 27. The descriptors making the largest contributions to the equation include: zagreb (an index describing the molecular connectivity and shape of the heavy atoms in the molecule); weight (the molecular weight of the compound); vsa\_hyd (a pharmacophore feature that approximates the sum of Van der Waal surface areas of hydrophobic atoms); and WeinerPath and WeinerPol (adjacency and distance matrix descriptors for path and polarity, respectively). Taken

TABLE 1

Compound number, R substituent, and  $\text{IC}_{50}$  value for inhibition of recombinant hNMT-1 by COPPs



Compound No.	–R	GST-hNMT-1 $\text{IC}_{50}$ $\mu\text{M}$
1	cyclohexyl	113 $\pm$ 7
2	3-pyridinyl	590 $\pm$ 127
3	2-methylbenzyl	121 $\pm$ 8
4	4-methoxybenzyl	419 $\pm$ 30
5	4-methylsulfanylbzyl	49 $\pm$ 13
6	4-methoxycarbonylbzyl	6400 $\pm$ 310
7	4-trifluoromethylbenzyl	44 $\pm$ 6
8	2-fluorobenzyl	>8000
9	2-nitrobenzyl	>8000
10	4-methoxy-3-methylbenzyl	284 $\pm$ 46
11	3,4-dimethoxybenzyl	240 $\pm$ 23
12	3,4-dichlorobenzyl	48 $\pm$ 5
13	2,6-dichlorobenzyl	77 $\pm$ 13
14	3,4-difluorobenzyl	89 $\pm$ 16
15	2,6-difluorobenzyl	6000 $\pm$ 250
16	4-methoxy-2,5-dimethylbenzyl	66 $\pm$ 13
17	5-bromo-2,4-dimethoxybenzyl	50 $\pm$ 2
18	2-bromo-4,5-dimethoxybenzyl	78 $\pm$ 1
19	2-nitro-4,5-dimethoxybenzyl	60 $\pm$ 6
20	2-naphthalenyl	42 $\pm$ 5
21	4-methoxy-naphthalene-1-ylmethyl	35 $\pm$ 5
22	2-methoxy-naphthalene-1-ylmethyl	28 $\pm$ 8
23	2-nitro-benzo[1,3]dioxol-1-ylmethyl	63 $\pm$ 15
24	9-ethyl-9H-carbazole-3-ylmethyl	6 $\pm$ 1
25	10b,10c-dihydro-pyrene-1-ylmethyl	70 $\pm$ 8
26	6-methyl-chromene-4-one-3-ylmethyl	>8000
27	4-bromo-thiophen-2-ylmethyl	>8000
28	5-(2-nitro-phenyl)-furan-2-ylmethyl	45 $\pm$ 2
29	5-(3-nitro-phenyl)-furan-2-ylmethyl	41 $\pm$ 1
30	5-(4-nitro-phenyl)-furan-2-ylmethyl	36 $\pm$ 4
31	2-(2,6,6-trimethyl-cyclohex-1-enyl)-ethyl	43 $\pm$ 4
32	3-(2-methoxy-phenyl)-allyl	1600 $\pm$ 200

together, these descriptors indicate that specific aspects of molecular size, shape, and polarity are critical determinants for inhibition of NMT.

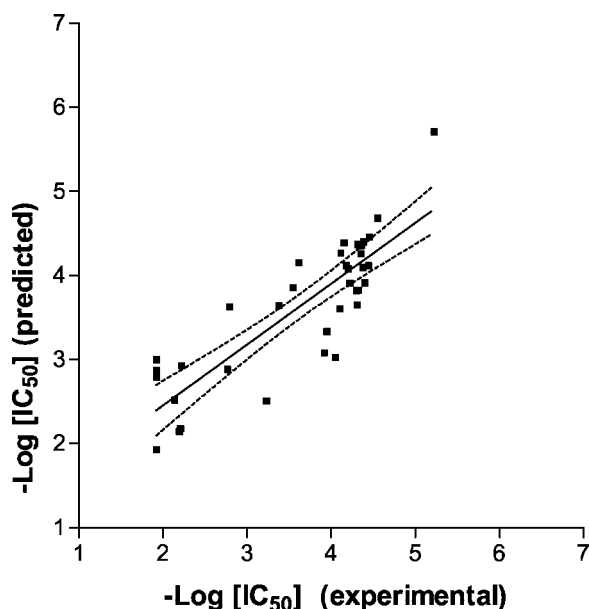
**Mechanism of Inhibition of NMT by COPP Compounds.** The mechanism of inhibition by the most potent COPP compound, 24, was examined using peptide and myristoyl-CoA substrate competition experiments with GST-hNMT-1. The results of these studies are summarized in Table 3. In the absence of inhibitor, the  $K_m$  for myristoyl-CoA compares very well with the literature value of 2.6  $\mu\text{M}$  (Rocque et al., 1993). The affinity of the enzyme for the biotinylated peptide is somewhat lower than the affinity of hNMT for the soluble peptide GNAASARR ( $K_m$ , 6  $\mu\text{M}$ ; Rocque et al., 1993). However, it is well established that the affinity for the peptide is highly sequence-sensitive, so that  $K_m$  values >100  $\mu\text{M}$  are not unusual. For studies of the ability of 24 to interact with the peptide-binding site of NMT, the peptide concentration was varied from 0 to 500  $\mu\text{M}$ , whereas the myristoyl-CoA concentration was kept constant in the assays. The presence of 24 at its  $\text{IC}_{50}$  concentration

TABLE 2

## QSAR parameters for inhibition of hNMT-1

Descriptor labels, correlation coefficients, and relative contributions of the 37 descriptors used in the optimized QSAR model are given. An explanation of the descriptor labels can be found at: [http://www.chemcomp.com/Journal\\_of\\_CCG/Features/descrip.html](http://www.chemcomp.com/Journal_of_CCG/Features/descrip.html).

Descriptor Label	Coefficient	Relative Importance
VdistMa	0.0161	0.004
WeinerPath	-2.0716	0.561
WeinerPol	-1.7817	0.483
A_count	0.3237	0.088
B_count	0.4147	0.112
chi0v	0.0739	0.020
chi0v_C	-0.1627	0.044
chi1v	-0.0267	0.007
chi1v_C	-0.3120	0.085
chi0	0.2606	0.071
chi0_C	-0.3518	0.095
chi1	0.2038	0.055
chi1_C	-0.5455	0.148
Weight	-1.8947	0.513
a_heavy	0.6767	0.183
a_nC	-0.4979	0.135
b_heavy	0.8628	0.234
VAdjEq	-0.0001	0.001
VAdjMa	0.0054	0.001
Zagreb	3.6917	1.000
PEOE_VSA_HYD	0.9180	0.249
Q_VSA_HYD	0.3018	0.082
Q_VSA_POS	-0.8456	0.229
Kier1	0.3802	0.103
KierA1	0.8288	0.224
Kier2	0.2431	0.151
Apol	0.9392	0.254
Mr	-0.0432	0.012
a_hyd	-0.9990	0.271
vsa_hyd	1.4436	0.391
SlogP	0.0965	0.026
SMR	-0.1007	0.027
SMR_VSA4	0.5563	0.151
SMR_VSA5	0.2381	0.065
vdw_area	-0.8456	0.229
vdw_vol	0.2737	0.074
LogP(o/w)	0.6595	0.179



**Fig. 3.** Regression analysis of QSAR model for predicting COPP potency. The experimental  $IC_{50}$  (Table 1) and the calculated  $IC_{50}$  for each of the 32 COPP and five MOPP compounds are shown. The best-fit linear regression line and 95% confidence intervals are shown.

TABLE 3

## Michaelis-Menten parameters for hNMT-1

Values represent the mean  $\pm$  S.D. for samples in one of three similar experiments.

Addition	Peptide		Myristoyl-CoA	
	$K_m$	$V_{max}$	$K_m$	$V_{max}$
	$\mu M$	$pmol/min$	$\mu M$	$pmol/min$
DMSO	$181 \pm 1$	$0.084 \pm 0.012$	$3.0 \pm 1.8$	$0.057 \pm 0.005$
6 $\mu M$ 24	$252 \pm 2$	$0.076 \pm 0.006$	$2.6 \pm 2.0$	$0.034 \pm 0.001$

decreased the  $K_m$  for the peptide relative to the solvent control. However, inhibition was overcome by the addition of excess peptide, as demonstrated by the similar  $V_{max}$  values, indicating that 24 acts as a competitive inhibitor with respect to the peptide substrate. To determine the effects of 24 on the myristoyl-CoA binding site, the concentration of myristoyl-CoA was varied from 0 to 100  $\mu M$ , whereas the peptide concentration was held constant in the assays. As shown in Table 3, the  $K_m$  for myristoyl-CoA was unchanged by the presence of 24. In contrast, the  $V_{max}$  decreased in the presence of 24, indicating that it acts as a noncompetitive inhibitor with respect to the lipid substrate. Overall, these kinetic analyses indicate that 24, and most likely the rest of the COPP family, inhibit NMT activity by competing with the substrate peptide for binding to the enzyme.

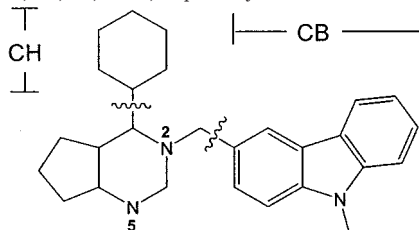
**Docking of COPP-24 to NMT.** The competition experiments described above provided important structural data that the COPP compounds interact with the peptide-binding site of hNMT-1. This was further explored using molecular modeling to develop a three-dimensional model of COPP interaction with NMT. Although the three-dimensional structure of human NMT remains to be determined, the structure of NMT from *S. cerevisiae* has been solved at 2.9 Å resolution (Bhatnagar et al., 1998). Sequence comparisons of human and yeast NMT indicate a very high level of sequence similarity. This homology is even more apparent in the active site, with residues involved in peptide binding being very highly conserved between the human and yeast isoforms. As shown in Table 4, 25 of the 26 residues that are involved in peptide binding are identical in the human isoform. Furthermore, 16 residues are absolutely conserved in all known NMT isoforms. Additionally, biochemical comparisons of the human and yeast enzymes have demonstrated that they share a degree of similarity (Rocque et al., 1993). Thus, the yeast NMT structure is likely to serve as an acceptable model until human NMT structure data are available.

As shown in Fig. 4A, the X-ray structure of the yeast NMT with bound myristoyl-CoA and peptide substrate analogs [*S*-(2-oxo)pentadecylCoA and SC-58272, respectively] was obtained from the Brookline Protein Data Bank (accession code 2nmt). The binding sites for the two substrates are in close proximity, and amino acid residues critical for providing the "oxyanion hole" that is necessary for polarization of the myristoyl-CoA amide have been identified (Bhatnagar et al., 1998). To determine the binding site for 24, SC-58272 was computationally removed, and hydrogen atoms were added to protein. Default parameter settings were used, and interaction energies for binding of 24 to a three-dimensional box encompassing the entire protein were calculated using a molecular mechanics force field (MMFF94) and simulated annealing and tabu search protocols. Both methods were set to optimize spatial contacts and electrostatic interactions. At

TABLE 4

Contact residues for SC-58272 and COPP-24

The models of NMT with bound peptide analog SC-58272 or COPP-24 were used to define amino acid residues in close proximity to these ligands. Residues within 3.0 Å of SC-58272 are indicated by an X. Residues within 3.0 Å of the cyclohexyl or carbazole groups, or 4.5 Å of the N<sup>2</sup> or N<sup>5</sup> groups of COPP-24 (as indicated below) are designated as CH, CB, N2, or N5, respectively.



Position	Residue	SC-58272	COPP-24
104**	Val	X	CH/N2
105**	Glu	X	N5
106**	Asp	X	CB/N2/N5
107*	Arg	X	N5
108*	Asp	X	
111*	Phe	X	CB
113**	Phe	X	
115**	Tyr	X	
169**	Asn	X	
205**	Thr	X	
206*	Ala	X	CH
207**	Gly	X	CH/N5
219**	Tyr	X	CH
221**	His	X	CB
223*	Pro	X	
234**	Phe	X	CB
235*	Thr	X	
334	Gly	X	CB
414**	Gly	X	
416**	Gly	X	CB
417**	Asp	X	CB
418**	Gly	X	CB/N2
419*	Phe		CH
420**	Leu	X	CH
454*	Met	X	
455*	Leu	X	

\* Residues conserved between the yeast and human isoforms.

\*\* Residues absolutely conserved in all known NMTs.

the end of each refinement cycle, acceptance tests were run until an optimal solution (lowest energy) was attained. After simulated annealing was run to convergence, the lowest-energy solution indicated that 24 binds to the enzyme in the peptide-binding groove very close to the catalytic residues. This is demonstrated in Fig. 4B, in which the protein has been hidden, leaving the myristoyl-CoA analog (left side) and an overlay of SC-58272 and 24 (right side). Compound 24 bound within the peptide-binding site in each iteration throughout the simulation. As shown, the COPP group binds near the site of the second and third residues of the peptide with the pyrrolo[1,2-*a*]pyrazine system positioned above and away from the peptide backbone, whereas the cyclohexyl moiety lies in the plane of the peptide substrate. This orientation appears to allow interaction of the cyclohexyl group with hydrophobic residues of NMT, and loss of this interaction probably explains the decreased activities of MOPP compounds in which a methyl group is substituted for the cyclohexyl moiety. Like the cyclohexyl group, the carbazole side chain of 24 lies in plane with the substrate peptide, extending through a large portion of the peptide-binding groove. This orientation may be further stabilized by the presence of aromatic residues of NMT, allowing in  $\pi$ -stacking interactions

with 24. This model suggests that the carbazole side chain is the most potent group tested, since it can closely interact with more NMT residues than smaller groups.

Analysis of the contact residues of NMT with the peptide analog or 24 indicated that 16 of the 25 residues of NMT that lie within 3 Å of the peptide analog are also shared with the modeled binding site for 24 (Table 4). There is only one residue (Phe-419) in close proximity to the binding site for 24 but not the peptide analog. It should be noted that the amino acid residues are numbered according to their position in the full-length yeast NMT protein, following the example of Bhatnagar (1998). Furthermore, of the 16 residues that are in close proximity to 24, 13 are absolutely conserved in all known NMT isoforms. These findings, in conjunction with the kinetic competition studies, indicate that the COPP compounds inhibit NMT activity by interacting with the peptide-binding site.

**Cellular Effects of COPP-24.** The assays described above demonstrate the ability of COPP-containing compounds to inhibit purified human NMT. To determine their efficacy in intact cells, a novel assay was developed in which the N terminus of GFP was modified to allow its myristoylation (*N*-myr-GFP) by endogenous NMT. This involves transient transfection of CV-1 cells with a plasmid encoding GFP to which a myristoylation signal patterned after that of the src family member Fyn (MGCVCQCKTK) is fused. This results in the myristoylation of the N-terminal glycine residue and the palmitoylation of a nearby cysteine residue, and these modifications of GFP target it to the plasma membrane (Fig. 5). Treatment of the *N*-myr-GFP-transfected cells with millimolar concentrations of a known, very low-potency inhibitor of NMT, 2-hydroxymyristic acid (2HM), resulted in redistribution of GFP to the cytosol. Similar effects are seen when the cells are treated with micromolar concentrations of 24, i.e., displacement of *N*-myr-GFP to the cytosol. The N-terminal sequence of the *N*-myr-GFP construct is different from the peptide substrate used in the screening assays, demonstrating that the COPP compounds can inhibit the myristoylation of a variety of proteins. This method provides evidence that the inhibitors detected in the screen with recombinant NMT can also block endogenous NMT activity in whole cells.

Since NMT is essential for the viability of yeast, and since several proliferative signaling pathways in cancer cells involve myristoylated proteins, the effects of 24 on the proliferation of a panel of human tumor cell lines were determined. As indicated in Table 5, 24 caused dose-dependent inhibition of the proliferation of a variety of tumor cell lines. The IC<sub>50</sub> values for 24 fell within a relatively narrow concentration range (0.9–14.8  $\mu$ M), suggesting that this class of compound may be useful for the treatment of tumors that derive from a variety of tissues. The compound also displayed sensitivity toward paired tumor and nontumor cells, as higher potency was observed in the human breast tumor cell line MCF-7 versus the nontumorigenic cell line MCF-10A. Of interest, colon-derived HT29 cells demonstrated increased sensitivity to 24, and previous work has indicated a close association of activation of Src (which requires myristoylation for activity) and colon cancer (Sawyer et al., 2001). Overall, the data indicate that 24 and, likely, related COPPs have excellent potential utility as anticancer agents.



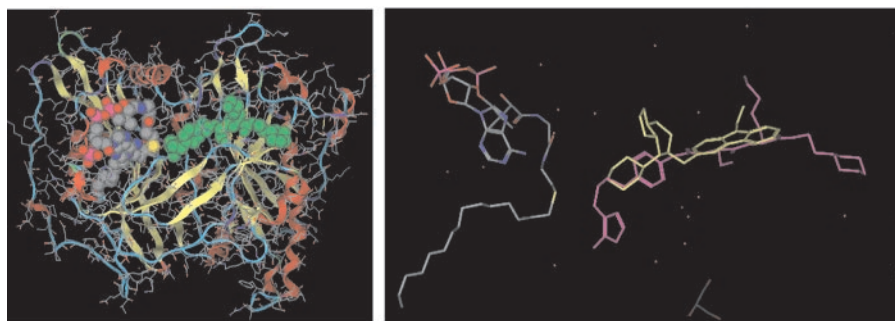


**Fig. 4.** Modeling of NMT interactions with 24. Left panel, the crystal structure of yeast NMT with bound myristoyl-CoA (left side) and SC-58272 (right side, green) substrate analogs. Right panel, protein-hidden model of binding of the myristoyl-CoA analog (left side) and an overlay of SC-58272 (magenta) and 24 (yellow) in the lowest total energy configuration.

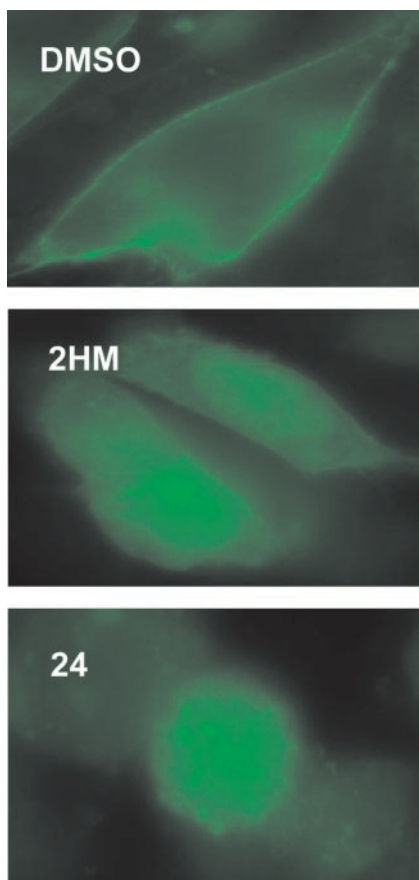


**Fig. 5.** Inhibition of endogenous NMT by 24. CV-1 monkey kidney cells were transfected with *N*-myr-GFP as described under *Materials and Methods*. The cells were treated with DMSO, 1 mM 2HM, or 4  $\mu$ M 24 for 48 h before the subcellular distribution of GFP was assessed by fluorescence microscopy. Images represent typical results in multiple experiments.

## Discussion

Because of the increasing evidence that protein *N*-myristoylation plays important roles in several pathogenic states, we sought to identify small-molecule inhibitors of human NMT. Previous drug development endeavors were aimed toward designing inhibitors specific toward fungal NMT activity (Masubuchi et al., 2001; Ebiike et al., 2002). We hypothesize that human NMT is an attractive target for cancer and viral therapeutics. To this end, we have developed an efficient assay for screening using recombinant human enzyme and a biotinylated substrate peptide and have identified a series of moderately potent inhibitors with activity both in vitro and with intact cells. The COPP chemotype consistently

**TABLE 5**

Cytotoxicity of 24 toward human tumor cell lines  
Values represent the mean  $\pm$  S.E.M. of four experiments.

Cell Line	Tissue of Origin	IC <sub>50</sub> $\mu$ M
DU145	Prostate	14.8 $\pm$ 2.9
HepG2	Liver	4.4 $\pm$ 1.2
HT29	Colon	3.7 $\pm$ 0.6
MCF-7	Breast	0.9 $\pm$ 0.3
MCF-10A B	Breast nontransformed	5.6 $\pm$ 2.9
MDA-MB-231	Breast	11.9 $\pm$ 1.3
Panc-1	Pancreas	12.6 $\pm$ 1.3
SKOV3	Ovary	13.2 $\pm$ 3.6
A-498	Kidney	5.8 $\pm$ 1.4

IC<sub>50</sub>, concentration of 24 that kills 50% of the cells.

demonstrated potency toward hNMT-1, indicating that it is an attractive scaffold for medicinal chemistry efforts. It is important to note that changing the substituent connected to the COPP nucleus markedly altered potency. For example, substitution of the 2-benzyl position with an electron-donating group (3) produced substantially more potent compounds than substitution with an electron-withdrawing group (8 and 9). Substitution of two fluorine atoms (15) for two chlorine atoms (13) greatly reduced the potency of the benzyl-substituted COPPs. In general, compounds with multiple conjugated ring systems were more potent than substituted benzyl, phenyl, or thiophenyl compounds. Overall, these results show that the COPP chemotype inhibits human NMT-1 activity at micromolar levels, and the structure of the side chain can dramatically influence activity. Further medicinal chemistry efforts will be required to achieve similar potencies as previously described peptidomimetics (Devadas et al., 1997) and nonhydrolyzable myristoyl-CoA analogs (Paige et al., 1989). Structure-activity relationships obtained from the screen revealed that most MOPP compounds showed no potency. However, there were several that inhibited hNMT-1 activity (data not shown). This is most likely due to the presence of potent side chains, which were not present in the initial COPP library. New COPP analogs will be synthesized that will incorporate these side chains and enrich the existing structure-activity relationship series.

Kinetic studies revealed that the most potent COPP-based inhibitor is competitive at the peptide-binding site of NMT. Since COPP 24 inhibition was removed with the addition of excess peptide substrate, it is unlikely that this chemotype is a false positive from the screen and is acting in a direct fashion. It may be desirable to target inhibitors toward the peptide-binding site for several reasons. Peptidomimetics tend to be more drug-like than analogs of the lipid substrate would be. However, peptidomimetics demonstrate poor inter-

tinal absorptive properties. Furthermore, lipids, such as the nonhydrolyzable myristoyl-CoA analogs, are poor drugs, demonstrating excessively rapid clearance, low volumes of distribution, and systemic toxicity. Experience with the development of inhibitors of farnesyltransferase has clearly demonstrated the advantage of peptidomimetics and bisubstrate analogs over farnesyl analogs. Finally, acyl-CoAs are substrates for a number of enzymes, and therefore, achieving selectivity for specific acyltransferases is likely to be difficult. The studies described herein provide methods and lead compounds for the development of inhibitors of human NMT. The COPP compounds, as small molecules, may achieve improved pharmacokinetic properties versus the peptidomimetic and lipid analogs described above. Continuing studies will seek to optimize these leads and to determine their in vivo therapeutic potential.

## References

- Bhatnagar RS, Futterer K, Farazi TA, Korolev S, Murray CL, Jackson-Machelski E, Gokel GW, Gordon JI, and Waksman G (1998) Structure of N-myristoyltransferase with bound myristoyl-CoA and peptide substrate analogs. *Nat Struct Biol* 5:1091–1097.
- Boutin JA (1997) Myristoylation. *Cell Signal* 9:15–35.
- Boutin JA, Clarenc JP, Ferry G, Ernould AP, Remond G, Vincent M, and Atassi G (1991) N-myristoyl-transferase activity in cancer cells. Solubilization, specificity and enzymatic inhibition of a N-myristoyl transferase from L1210 microsomes. *Eur J Biochem* 201:257–263.
- Boutin JA, Ferry G, Ernould AP, Maes P, Remond G, and Vincent M (1993) Myristoyl-CoA:protein N-myristoyltransferase activity in cancer cells. Purification and characterization of a cytosolic isoform from the murine leukemia cell line L1210. *Eur J Biochem* 214:853–867.
- Chow M, Newman JF, Filman D, Hogle JM, Rowlands DJ, and Brown F (1987) Myristylation of picornavirus capsid protein VP4 and its structural significance. *Nature (Lond)* 327:482–486.
- Cordo SM, Candurra NA, and Damonte EB (1999) Myristic acid analogs are inhibitors of Junin virus replication. *Microbes Infect* 1:609–614.
- Devadas B, Freeman SK, Zupce ME, Lu HF, Nagarajan SR, Kishore NS, Lodge JK, Kuneman DW, McWherter CA, Vinjamoori DV, et al. (1997) Design and synthesis of novel imidazole-substituted dipeptide amides as potent and selective inhibitors of *Candida albicans* myristoyl-CoA:protein N-myristoyltransferase and identification of related tripeptide inhibitors with mechanism-based antifungal activity. *J Med Chem* 40:2609–2625.
- Devadas B, Zupce ME, Freeman SK, Brown DL, Nagarajan S, Sikorski JA, McWherter CA, Getman DP, and Gordon JI (1995) Design and syntheses of potent and selective dipeptide inhibitors of *Candida albicans* myristoyl-CoA:protein N-myristoyltransferase. *J Med Chem* 38:1837–1840.
- Duronio RJ, Rudnick DA, Johnson RL, Johnson DR, and Gordon JI (1991) Myristic acid auxotrophy caused by mutation of *S. cerevisiae* myristoyl-CoA:protein N-myristoyltransferase. *J Cell Biol* 113:1313–1330.
- Duronio RJ, Towler DA, Heuckeroth RO, and Gordon JI (1989) Disruption of the yeast N-myristoyl transferase gene causes recessive lethality. *Science (Wash DC)* 243:796–800.
- Ebiike H, Masubuchi M, Liu P, Kawasaki K, Morikami K, Sogabe S, Hayase M, Fujii T, Sakata K, Shindoh H, et al. (2002) Design and synthesis of novel benzofurans as a new class of antifungal agents targeting fungal N-myristoyltransferase. Part 2. *Bioorg Med Chem Lett* 12:607–610.
- Furuishi K, Matsuoka H, Takama M, Takahashi I, Misumi S, and Shoji S (1997) Blockage of N-myristoylation of HIV-1 gag induces the production of impotent progeny virus. *Biochem Biophys Res Commun* 237:504–511.
- Garcia R, Bowman TL, Niu G, Yu H, Minton S, Muro-Cacho CA, Cox CE, Falcone R, Fairclough R, Parsons S, et al. (2001) Constitutive activation of Stat3 by the Src and JAK tyrosine kinases participates in growth regulation of human breast carcinoma cells. *Oncogene* 20:2499–2513.
- Giang DK and Cravatt BF (1998) A second mammalian N-myristoyltransferase. *J Biol Chem* 273:6595–6598.
- Heuckeroth RO and Gordon JI (1989) Altered membrane association of p60v-src and a murine 63-kDa N-myristoyl protein after incorporation of an oxygen-substituted analog of myristic acid. *Proc Natl Acad Sci USA* 86:5262–5266.
- Kamps MP, Buss JE, and Sefton BM (1986) Rous sarcoma virus transforming protein lacking myristic acid phosphorylates known polypeptide substrates without inducing transformation. *Cell* 45:105–112.
- Likhoshershtov AM, Peresada VP, and Skoldinov AP (1993) New route to the synthesis of octahydropyrrolo[1, 2-a] pyrazines. *Khim-Farm Zh* 27:46–48.
- Lodge JK, Jackson-Machelski E, Toffaletti DL, Perfect JR, and Gordon JI (1994) Targeted gene replacement demonstrates that myristoyl-CoA: protein N-myristoyltransferase is essential for viability of *Cryptococcus neoformans*. *Proc Natl Acad Sci USA* 91:12008–12012.
- Masubuchi M, Kawasaki K, Ebiike H, Ikeda Y, Tsujii S, Sogabe S, Fujii T, Sakata K, Shiratori Y, Aoki Y, et al. (2001) Design and synthesis of novel benzofurans as a new class of antifungal agents targeting fungal N-myristoyltransferase. Part 1. *Bioorg Med Chem Lett* 11:1833–1837.
- McIlhinney RA, Young K, Egerton M, Camble R, White A, and Soloviev M (1998) Characterization of human and rat brain myristoyl-CoA:protein N-myristoyltransferase: evidence for an alternative splice variant of the enzyme. *Biochem J* 333:491–495.
- Nagarajan SR, Devadas B, Zupce ME, Freeman SK, Brown DL, Lu HF, Mehta PP, Kishore NS, McWherter CA, Getman DP, et al. (1997) Conformationally constrained [p-(omega-aminoalkyl)phenacetyl]-L-seryl-L-lysyl dipeptide amides as potent peptidomimetic inhibitors of *Candida albicans* and human myristoyl-CoA: protein N-myristoyl transferase. *J Med Chem* 40:1422–1438.
- Paige LA, Zheng GQ, DeFrees SA, Cassidy JM, and Geahlen RL (1989) S-(2-oxopentadecyl)-CoA, a nonhydrolyzable analogue of myristoyl-CoA, is a potent inhibitor of myristoyl-CoA:protein N-myristoyltransferase. *J Med Chem* 32:1665–1667.
- Rajala RV, Radhi JM, Kakkar R, Datla RS, and Sharma RK (2000) Increased expression of N-myristoyltransferase in gallbladder carcinomas. *Cancer* 88:1992–1999.
- Raju RV, Datla RS, and Sharma RK (1996) Expression of human N-myristoyltransferase in *Escherichia coli*. Comparison with N-myristoyltransferases expressed in different tissues. *Mol Cell Biochem* 155:69–76.
- Raju RV, Moyana TN, and Sharma RK (1997) N-Myristoyltransferase overexpression in human colorectal adenocarcinomas. *Exp Cell Res* 235:145–154.
- Resh MD (1994) Myristylation and palmitylation of Src family members: the fats of the matter. *Cell* 76:411–413.
- Resh MD (1996) Regulation of cellular signalling by fatty acid acylation and prenylation of signal transduction proteins. *Cell Signal* 8:403–412.
- Robbins SM, Quintrell NA, and Bishop JM (1995) Myristoylation and differential palmitoylation of the HCK protein-tyrosine kinases govern their attachment to membranes and association with caveolae. *Mol Cell Biol* 15:3507–3515.
- Rocque WJ, McWherter CA, Wood DC, and Gordon JI (1993) A comparative analysis of the kinetic mechanism and peptide substrate specificity of human and *Saccharomyces cerevisiae* myristoyl-CoA:protein N-myristoyltransferase. *J Biol Chem* 268:9964–9971.
- Rudnick DA, McWherter CA, Rocque WJ, Lennon PJ, Getman DP, and Gordon JI (1991) Kinetic and structural evidence for a sequential ordered Bi Bi mechanism of catalysis by *Saccharomyces cerevisiae* myristoyl-CoA:protein N-myristoyltransferase. *J Biol Chem* 266:9732–9739.
- Sawyer T, Boyce B, Dalgarno D, and Iulucci J (2001) Src inhibitors: genomics to therapeutics. *Expert Opin Investig Drugs* 10:1327–1344.
- Skehan P, Storeng R, Scudiero D, Monks A, McMahon J, Vistica D, Warren JT, Bokesch H, Kenney S, and Boyd MR (1990) New colorimetric cytotoxicity assay for anticancer-drug screening. *J Natl Cancer Inst* 82:1107–1112.
- Song KS, Sargiacomo M, Galbati F, Parenti M, and Lisanti MP (1997) Targeting of a G alpha subunit (Gi1 alpha) and c-Src tyrosine kinase to caveolae membranes: clarifying the role of N-myristoylation. *Cell Mol Biol (Noisy-Le-Grand)* 43:293–303.
- Tabuchi M, Okamoto H, Furutani T, Azuma M, Ooshima H, Otake T, Kawahata T, and Kato J (1997) Inhibition of octapeptide N-myristoylation by acyl amino acids and acyl alkanolamines. *J Enzyme Inhib* 12:27–36.
- van't Hof W and Resh MD (1999) Dual fatty acylation of p59(Fyn) is required for association with the T cell receptor zeta chain through phosphotyrosine-Src homology domain-2 interactions. *J Cell Biol* 145:377–389.
- Wagner AP and Retey J (1991) Synthesis of myristoyl-carba(dethia)-coenzyme A and S-(3-oxohexadecyl)-coenzyme A, two potent inhibitors of myristoyl-CoA:protein N-myristoyltransferase. *Eur J Biochem* 195:699–705.
- Weinberg RA, McWherter CA, Freeman SK, Wood DC, Gordon JI, and Lee SC (1995) Genetic studies reveal that myristoyl-CoA:protein N-myristoyltransferase is an essential enzyme in *Candida albicans*. *Mol Microbiol* 16:241–250.
- Yurchak LK and Sefton BM (1995) Palmitoylation of either Cys-3 or Cys-5 is required for the biological activity of the Lck tyrosine protein kinase. *Mol Cell Biol* 15:6914–6922.
- Zha J, Weiler S, Oh KJ, Wei MC, and Korsmeyer SJ (2000) Posttranslational N-myristoylation of BID as a molecular switch for targeting mitochondria and apoptosis. *Science (Wash DC)* 290:1761–1765.
- Zheng J, Knighton DR, Xuong NH, Taylor SS, Sowadski JM, and Ten Eyck LF (1993) Crystal structures of the myristylated catalytic subunit of cAMP-dependent protein kinase reveal open and closed conformations. *Protein Sci* 2:1559–1573.

**Address correspondence to:** Dr. Charles D. Smith, Department of Pharmacology, H078, Penn State College of Medicine, Hershey, PA 17033. E-mail: cdsmith@psu.edu